JEE Journal of Ecological Engineering

Journal of Ecological Engineering, 2026, 27(6), 213–224
https://doi.org/10.12911/22998993/216711
ISSN 2299–8993, License CC-BY 4.0

Received: 2025.11.28
Accepted: 2026.04.16
Published: 2026.05.01

Study adsorption of Fe(II) by spent bleaching earth chitosan crosslinked epichlorohydrin composite

Umi Baroroh Lili Utami[1,2*], Utami Irawati[2], Abdulah[2], Muhammad Syahirul Alim[3]

[1] Environmental Studies Program, Postgraduate Study School, Lambung Mangkurat University Banjarmasin, Indonesia
[2] Chemistry Departement, Faculty of Mathematics and Sains, Lambung Mangkurat University Banjarmasin, Indonesia
[3] Department of Environmental Engineering, Faculty of Engineering, Lambung Mangkurat University Banjarmasin, Indonesia
* Corresponding author's e-mail: umi.baroroh@ulm.ac.id

ABSTRACT

Spent bleaching earth (SBE) is a solid waste generated from the crude palm oil (CPO) bleaching process. SBE has potential as an adsorbent; however, its adsorption capacity is relatively limited and requires enhancement. In this study, the adsorption capacity of SBE was improved by compositing it with chitosan. To enhance the stability of the adsorbent, the SBE–chitosan composite was crosslinked using epichlorohydrin (ECH). The resulting ECH-crosslinked SBE–chitosan composite was evaluated for its ability to adsorb Fe(II) heavy metal ions. Fourier transform infrared spectroscopy (FTIR) was employed to confirm the successful formation of the composite. Infrared spectra revealed interactions between the ECH-crosslinked SBE–chitosan composite and Fe(II) ions, indicated by shifts in wavenumbers and the appearance of new functional groups The results indicated that the composite was successfully synthesized, as evidenced by FTIR analysis. Optimal adsorption occurred at pH 5 with a contact time of 110 minutes. The adsorption behavior of the composite was Langmuir and Freundlich isotherm model, and the maximum adsorption capacity determined from Langmuir model was 11.23 mgg^{-1}.

Keywords: spent bleaching earth, chitosan, epichlorohydrin, adsorption, Fe(II).

INTRODUCTION

Heavy metals are one of the most important contaminants in water and soil. Heavy metals are discharged into the environment by several industries, such as mining, metallurgy, electronics, electroplating and metal finishing [1]. Wastewater from coal-mining operations has been found to contain Fe and other heavy metals above environmental quality standards [2], groundwater contamination with Fe and Mn has been reported in mining regions, where concentrations greatly exceed safe drinking-water thresholds aising concerns over long-term human health effects [3]. Acid mine drainage (AMD), characterized by low pH and high concentrations of sulfate and heavy metals, results from the oxidation of sulfide minerals commonly found in the parent rocks of various ore deposits [4]. This acidic water causes environmental damage, especially as sulfuric acid dissolves heavy metals like arsenic, copper, lead, iron, and manganese [5]. Research conducted at PT Jorong Barutama Greston showed that manganese concentrations ranged from 8.3 mg/L to 21.75 mg/L, exceeding the standard of 4 mg/L, and iron concentrations ranged from 10.32 mg/L to 41.97 mg/L, surpassing the standard of 7 mg/L [6, 7]. To reduce heavy metal pollution, especially AMD, which contains high Fe, an adsorbent is needed that is resistant to acidic conditions and can absorb metals.

One promising adsorbent material is SBE, a waste product from the decolorization process in CPO refining. SBE is the largest waste stream in the industry, accounting for 0.5–2.0% of the total processed CPO mass. However,

SBE has limited adsorption capacity and thus requires reactivation to enhance its adsorption performance [8–11]. Moreover, SBE cannot be reused multiple times, necessitating its combination with other materials such as chitosan. Chitosan, a polymer with amine (-NH_2) and hydroxyl (-OH) groups along its chain, is effective in binding heavy metal ions [12–15]. However, chitosan has a limitation as an adsorbent due to its instability under acidic conditions [16]. One approach to this modification is through crosslinking [17]. The amino mer chains which are positively charged fall apart in solution groups in chitosan are fully protonated at pH ~3, and the poly- resulting in dissolution [18]. In order to enhance the resistance of chitosan against acid, alkali and chemicals as well as increasing chitosan adsorption ability and mechanical strength, crosslinking reaction is a crucial step [19]. Different kinds of crosslinking agents such as glutaraldehyde [20], epichlorohydrin and ethylene glycol diglycidyl ether [21].

Previous research has shown that epichlorohydrin (ECH) as a crosslinking agent has good properties. The optimum concentration of 5% ECH for chitosan beads was achieved. The adsorption of Zn(II) by chitosan–water hyacinth charcoal crosslinked with ECH at pH 4 reached 87.1% [22]. Epichlorohydrin (ECH) crosslinking chitosan with ECH offers the advantage that the amine groups in chitosan are still present, and the covalent bonds formed produce a stronger and more stable structure [23]. In this process, the hydroxyl carbon atom of chitosan forms covalent bonds that lead to the opening of the ECH epoxide ring and the release of chlorine atoms [24, 25]. The incorporation of SBE material with chitosan is aimed at enhancing the adsorption capacity of SBE. Research on isotherm studies of SBE, chitosan and ECH has been carried out extensively, including on SBE in dyes, where, the adsorption mechanism was in accordance with the Langmuir isotherm model [26]. Adsorption of humic acid on crosslinked chitosan–epichlorohydrin (chitosan–ECH) beads was equilibrium isotherms were analyzed by Langmuir and Freundlich models. Freundlich model was found to show the best fit for experimental data while the maximum adsorption capacity determined from Langmuir model was 44.84 mg/g [27]. Therefore, research is needed on the synthesis of composite SBE-chitosan-and ECH, and a study of the adsorption of the composite to Fe at pH, contact time, and isotherm.

MATERIALS AND METHODS

Instruments and materials

The instruments employed in this study included an analytical balance, filter paper, 100-mesh sieve, mortar and pestle, standard laboratory glassware, universal indicator, oven, furnace, Soxhlet apparatus, hotplate, Fourier Transform Infrared (FTIR 8201PC Shimadzu) Spectrophotometer, and Atomic Absorption Spectroscopy (AAS-GBC Avanta Ω). The materials utilized comprised SBE, commercial chitosan (degree of deacetylation 97.03%), 16 M nitric acid (HNO_3), distilled water, technical grade acetone, concentrated acetic acid (99%), ferrous sulfate heptahydrate ($FeSO_4 \cdot 7H_2O$) crystals, 37% hydrochloric acid (HCl), solid sodium hydroxide (NaOH), and epichlorohydrin (ECH).

Procedure

Preparation of spent bleaching earth (SBE)

SBE was ground using a mortar and pestle and sieved to obtain particles passing through a 100-mesh sieve. Oil extraction was performed using a Soxhlet apparatus with acetone as the solvent. Specifically, 50 gs of the ground SBE were placed into a thimble, which was subsequently inserted into the Soxhlet extractor. Approximately 500 mL of acetone was added, and the extraction process was conducted at 72 °C for 8 hours.

Activation of spent bleaching earth (SBE)

The activation process involved treatment with 0.8 M HNO_3 solution. A mixture of SBE and HNO_3 solution at a ratio of 1:10 (g/mL) was stirred using a magnetic stirrer at 70 °C and 300 rpm for 1 hour. The resulting solid residue was thoroughly washed with distilled water and dried in an oven at 105 °C for 24 hours. Subsequently, the material underwent carbonization in a furnace at 500 °C for 2 hours [28]. Characterization of SBE before and after activation was conducted using FTIR.

Synthesis of spent bleaching earth (SBE)-chitosan composite

10 gs of chitosan were dissolved in 100 mL of 2% (w/v) acetic acid solution and stirred with a magnetic stirrer until a viscous and homogeneous solution was formed. The SBE-chitosan composite was prepared by mixing SBE and chitosan at a weight ratio of 4:1 (w/w). The formed composite, appearing in pellet form, was dried in an oven at 70–80 °C. Both the chitosan and SBE-chitosan composites were characterized using FTIR.

Synthesis of SBE- chitosan crosslinked epichlorohydrin composite

5% (v/v) ECH solution was prepared and adjusted to pH 10 using a 0.067 M NaOH solution. Subsequently, 3.125 gs of the SBE-chitosan composite were mixed with 6.25 mL of the ECH solution and stirred magnetically for 70 minutes. The procedure was repeated for ECH concentrations of 5%, 7.5%, 10%, and 12.5%. The resulting crosslinked composites were filtered and washed with distilled water to remove residual ECH. The crosslinked composites were then analyzed using FTIR.

Effect of pH on adsorption

Solutions of $FeSO_4 \cdot 7H_2O$ at a concentration of 46.31 ppm were prepared and adjusted to pH values of 1, 3, 5, 7, and 9 using 0.1 M HCl or 0.1 M NaOH. A total of 3.125 gs of adsorbent and 100 mL of $FeSO_4 \cdot 7H_2O$ solution were placed in individual Erlenmeyer flasks and stirred with a magnetic stirrer for 70 minutes. After filtration, the concentration of iron in the filtrate was determined using AAS.

Effect of contact time on adsorption

A total of 3.125 g of adsorbent and 100 mL of 46.31 ppm $FeSO_4 \cdot 7H_2O$ solution were placed in individual Erlenmeyer flasks and stirred magnetically for various contact times of 30, 50, 70, 90, and 110 minutes. The experiments were conducted at the optimum pH determined previously. The filtrate obtained after filtration was analyzed by AAS.

Determination of adsorption capacity

Adsorption capacity was determined under the optimum pH and contact time conditions. $FeSO_4 \cdot 7H_2O$ solutions with concentrations of 11.50, 22.80, 33.71, 46.31, and 55.55 ppm were prepared. A total of 3.125 g of adsorbent was added to 250 mL Erlenmeyer flasks containing 46.31 ppm and 55.55 ppm $FeSO_4 \cdot 7H_2O$ solutions, and the mixtures were stirred with a magnetic stirrer for 50 minutes. After filtration, the filtrates were analyzed for iron content using AAS.

Data analysis

The Langmuir adsorption isotherm equation can be written as follows:

$$\frac{C_e}{q_e} = \frac{1}{q_{max} K_L} + \frac{1}{q_{max}} C_e \quad (1)$$

where: q_e is the amount of adsorbate adsorbed at equilibrium (mg/g), C_e is the equilibrium concentration of the solution (mg/L), K_L is the Langmuir constant related to the adsorption energy (L/mg), which is determined from the slope and intercept of the linear plot of C_e/q_e versus C_e, and q_{max} represents the maximum adsorption capacity of the adsorbent (mg/g).

The Freundlich adsorption isotherm equation is expressed as follows:

$$Log\ q_e = log\ K_F + \frac{1}{n} log\ C_e \quad (2)$$

where: q_e is the amount of adsorbate adsorbed at equilibrium (mg/g), C_e is the equilibrium concentration of the solution (mg/L), and (K_F) and (1/n) are the Freundlich constants representing the adsorption capacity and adsorption intensity, respectively.

RESULTS AND DISCUSSION

Activation of spent bleaching earth

The identification of functional groups in the infrared spectra of SBE powder, Soxhlet-extracted SBE, and activated SBE can be seen in Figure 1. The identification of each functional group in the infrared spectra of raw SBE powder, Soxhlet-extracted SBE, and activated SBE (c) can be seen in Table 1.

The infrared spectrum results on the characteristics of SBE powder have symmetric O-H stretching vibration functional groups between layers at wave numbers 3400–3650 cm^{-1}. At 2921.20 cm^{-1} and 2852.10 cm^{-1} are symmetric aliphatic CH_2 and asymmetric stretching vibrations, after the calcination process, these absorption

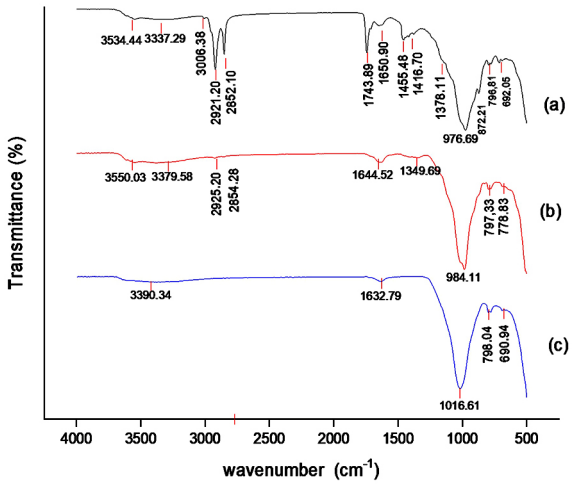

Figure 1. (a) Infrared spectrum of raw spent bleaching earth (SBE) powder, (b) Soxhlet-extracted SBE, and (c) activated SBE

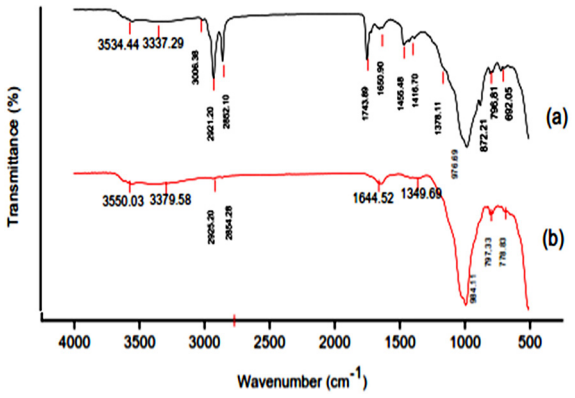

Figure 2. FTIR spectrum of the (a) SBE-chitosan and (b) SBE-chitosan crosslinked epichlorohydrin

bands disappear, which is direct evidence that the remains of organic matter have been converted into carbon species during the heating process (Tang et al., 2015). At 1743.89 cm^{-1} to 1455.48 cm^{-1} indicate the presence of C=O bonds and C=C or O-H bonds, which represent unsaturated vegetable oils in SBE [30]. These peaks disappear in the soxhleted SBE, as shown in Figure 3b, due to the soxhlet extraction of oil residues in SBE from the surface and inner pores of SBE. The aliphatic CH_2 group during soxhletation decreased in intensity and disappeared upon activation. This is because the aliphatic group was activated using HNO_3 to remove organic impurities and heated in a furnace at 500 °C, causing the aliphatic CH_2 to evaporate and become undetectable in the infrared spectrum in Figure 3c. The characteristic peaks of bleaching earth are present at 1060 cm^{1} and 800 cm^{-1} and indicate the silicate (Si-O) and silica/quartz (Si-O bending vibration in kaolinite) matrices are maintained throughout the sample, respectively, as shown in Figure 3, confirming that bleaching earth maintains its core matrix during extraction [30]. FTIR results also show a characteristic absorption peak at 1640 cm^{-1}, indicating the presence of structural water in the matrix or hydroxyl bending vibrations.

Synthesis of epichlorohydrin crosslinked chitosan-SBE composite

Characterized Fourier transform infrared (FTIR) shown in Figure 2. In Figure 2a, the IR spectrum of the SBE–chitosan composite shows an absorption peak at a wavenumber of 3242.81 cm^{-1}, corresponding to the stretching vibration of hydroxyl groups (–OH). When the SBE–chitosan composite is crosslinked with epichlorohydrin, the –OH group shifts from 3242.81 cm^{-1} to 3261.39 cm^{-1}. This shift is attributed to the interaction between the methylene group of epichlorohydrin and the primary –OH group of chitosan, causing

Table 1. Identification of functional groups in the infrared spectra of spent bleaching earth (SBE), Soxhlet-extracted SBE, and activated SBE [29]

Spent bleaching earth (SBE) (cm^{-1})	Spent bleaching earth (SBE)-0.8M HNO_3	Spent bleaching earth (SBE) 0.8M HNO_3, 500 °C	Reference wavenumber (cm^{-1})**	Fungcional group**
3534.44	3550.03	3390.34	3412–3100	Symmetric stretching vibration O-H
2921.20 & 2852.10	2925.20 & 2854.28	-	2924–2855	Symmetric stretching vibration CH and acymetric CH_2 alifatic
1743	-	-	1745–1700	C=O
1650.90	1644.52	1632.79	1650–1600	O-H
976.69	1349.69	1016.16	1040–1070	Si-O-Si
796.81	797.33	798.04	780–797	Silica amorf

an overlap with the original –OH stretching band at 3242.81 cm^{-1} [31–33]. Figure 2b an absorption peak at 1582.38 cm^{-1} is assigned to the N–H bending and stretching vibrations of amine groups ($–NH_2$) present in chitosan. Characteristic bands corresponding to the Spent Bleaching Earth (SBE) matrix are observed at 1013.88 cm^{-1} and 776.00 cm^{-1}, which are attributed to Si–O stretching and Si–O bending vibrations of silicate and silica/quartz frameworks, respectively [34]. The proposed structural interaction mechanism between SBE-chitosan and epichlorohydrin is illustrated in Figure 3. In this mechanism, chitosan acts as the main polymer with amino ($–NH_2$) and hydroxyl (−OH) groups at several positions along its chain. Epichlorohydrin functions as a linker, enabling crosslinking between the chitosan chains and interacting with the silanol (−Si−OH) groups present on the silica surface The interaction between chitosan and silica, mediated by epichlorohydrin, results in a stable network. This structure strengthens the composite and improves its chemical stability and mechanical strength while preserving the adsorption capability of the amino groups on chitosan and silica. This composite is ideal for the adsorption of Fe(II) metal ions [35].

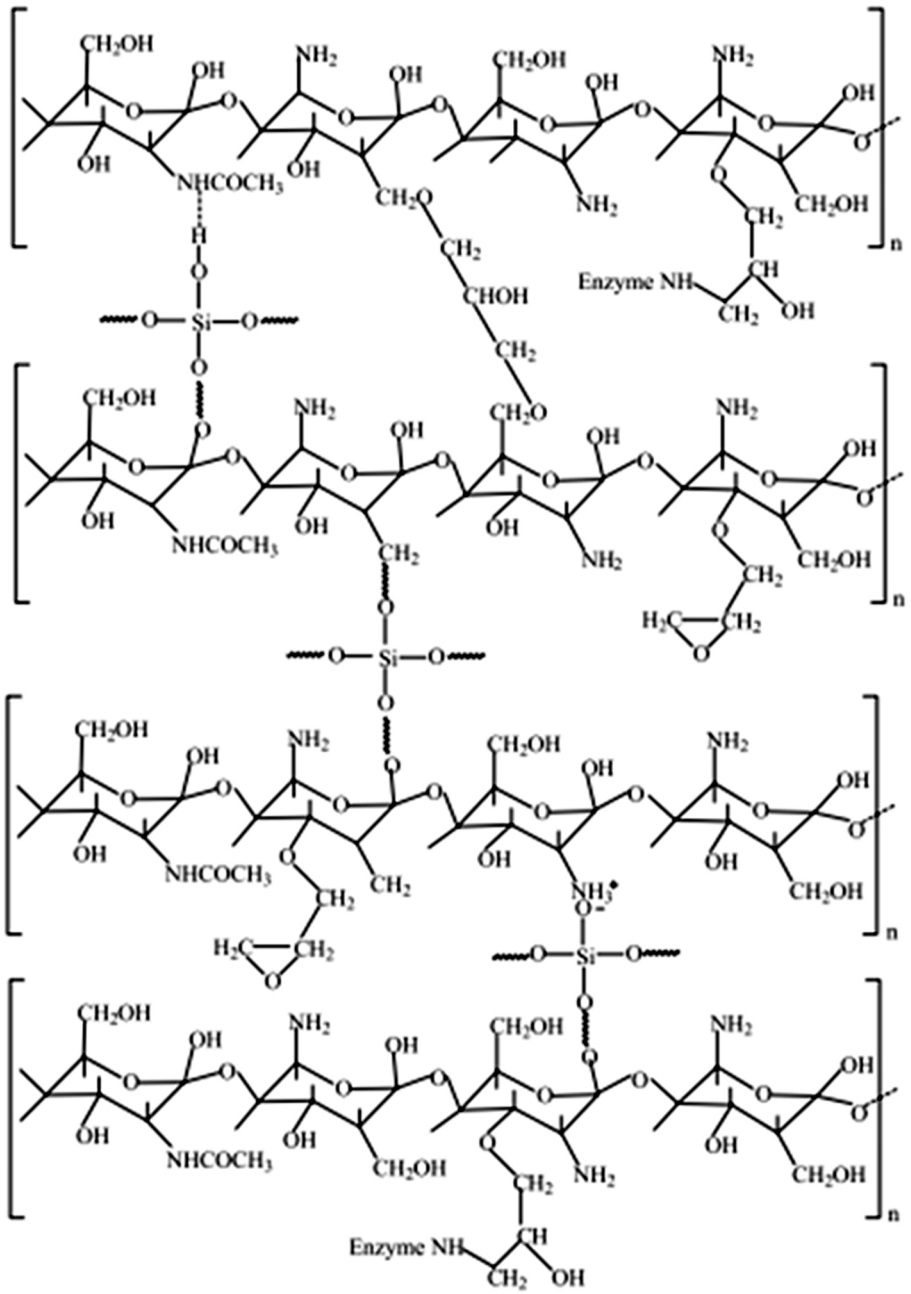

Figure 3. Structural mechanism of SiO_2-chitosan with epichlorohydrin [35]

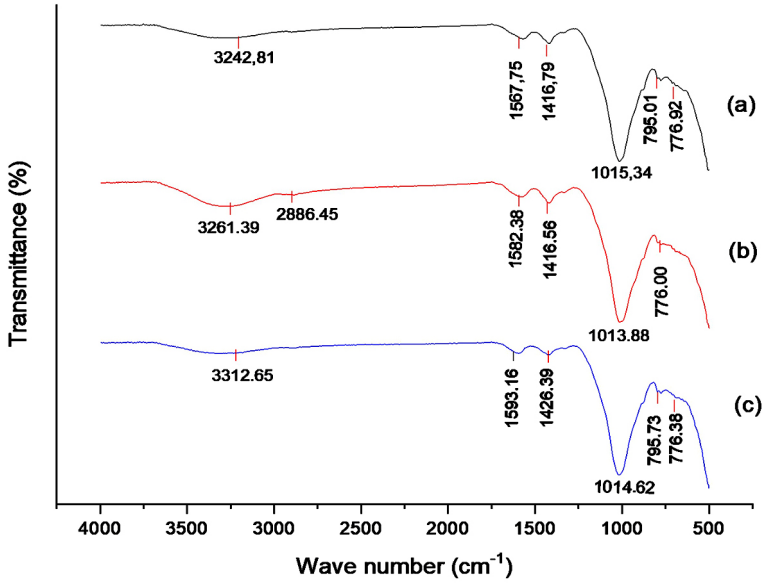

Figure 4. FTIR Spectrum of the SBE-chitosan crosslinked epichlorohydrin (a), SBE-chitosan composite, the SBE-chitosan composite cross-linked with epichlorohydrin (b), and the SBE-chitosan composite cross-linked with epichlorohydrin after adsorption Fe(II) (c)

Identification of functional groups in the infrared spectra of SBE-chitosan composites, SBE-chitosan crosslinked with epichlorohydrin composites, and SBE-chitosan crossinked with epichlorohydrin composites after adsorbing Fe(II) metal, can be seen in Figure 4. Identification of each functional group in the infrared spectra of the SBE-chitosan composite, the SBE-chitosan composite cross-linked with epichlorohydrin, and the SBE-chitosan composite cross-linked with epichlorohydrin after adsorbing Fe(II) can be seen in Table 2.

Based on Figure 4a, the IR spectrum of the SBE–chitosan composite shows an absorption peak at a wavenumber of 3242.81 cm^{-1}, corresponding to the stretching vibration of hydroxyl groups (–OH). When the SBE–chitosan composite is crosslinked with epichlorohydrin, the –OH group shifts from 3242.81 cm^{-1} to 3261.39 cm^{-1}. This shift is attributed to the interaction between the methylene group of epichlorohydrin and the primary –OH group of chitosan, causing an overlap with the original –OH stretching band at 3242.81 cm^{-1} [36]. In Figure 4(b), the C-H stretching vibration of epichlorohydrin appears at 2886.45 cm^{-1} after the crosslinking process [37]. The IR spectrum at 1567.75 cm^{-1} for the SBE–chitosan composite shows a primary amide (C=O) vibration, indicating the presence of residual acetyl groups even after crosslinking, as shown in Figure 4c, which also displays amide and amine ($–NH_2$) functional groups.

Table 2. Identification of functional groups in the infrared spectra of SBE-chitosan composites, SBE-chitosan composites cross-linked with epichlorohydrin, and SBE-chitosan composites cross-linked with epichlorohydrin after adsorption Fe(II) [29]

SBE-chitosan (cm^{-1})	SBE-chitosan-ECH	SBE-chitosan-ECH-Fe(II)	Wave number reference (cm^{-1})**	Functional group **
3242.81	3261.39	3312.65	3500–3200	–OH
-	2886.45	-	2872–2962	CH from CH_2
1567.75	1582.38	1593.16	1640–1540	Stretch vibration −NH from–NH_2
1416.79	1416.56	1426.39	1475–1300	Alkyl bending vibration C-H
1015.34	1013.88	1014.62	1016.03–1010.58	Asymmetric Si-O group stretching vibration
795.01	776.00	795.73	780–797	Vibration of amorphous silica
776.92	776.00	776.38	750–800	Symmetrical Si-O-Si bending vibration

In the epichlorohydrin-crosslinked SBE–chitosan composite, a new absorption appears at 1604.77 cm^{-1}. According to Table 2, the infrared spectrum shows a shift in the –OH functional group from 3242.81 cm^{-1} to 3261.39 cm^{-1} in the crosslinked composite, indicating interaction between SBE–chitosan and epichlorohydrin. The absorption band at 1567.75 cm^{-1}, associated with $–NH_2$ groups, shifts to 1582.38 cm^{-1}, suggesting the involvement of $–NH_2$ in the crosslinking reaction. This occurs because the –OH groups on the SBE–chitosan composite are utilized for crosslinking with epichlorohydrin. Furthermore, interaction between the epichlorohydrin-crosslinked SBE–chitosan composite and Fe(II) ions is indicated by a wavenumber shift from 1582.38 cm^{-1} to 1593.15 cm^{-1}, showing that the $–NH_2$ groups interact with Fe(II). This is due to the lone pair electrons on the $–NH_2$ group that can coordinate with Fe(II) cations through coordinate bonding.

Determination of the adsorption Fe(II) by SBE-chitosan crosslinked epichlorohydrin composites

The adsorption of Fe(II) was conducted using SBE- chitosan crosslinked epichlorohydrin- composites with varying epichlorohydrin concentrations of 5%, 7.5%, 10%, and 12.5%. The adsorption of Fe(II) at a concentration of 46.31 ppm was carried out under optimum conditions based at pH 5 and a contact time of 70 minutes [38]. The optimum concentration of epichlorohydrin was determined by observing the highest adsorption percentage, as the concentration of epichlorohydrin (ECH) that produced the greatest adsorption indicated the best condition for metal binding by the adsorbent. The results of the adsorption percentage at various epichlorohydrin concentrations are shown in Figure 5.

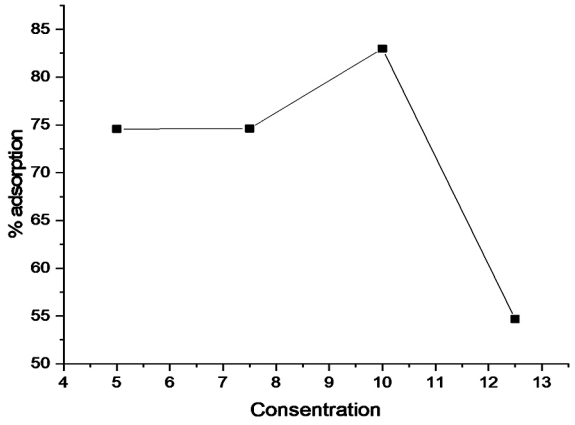

Figure 5. Graph of the effect of epichlorohydrin concentration (%) on epichlorohydrin-crosslinked SBE-chitosan composite for Fe(II) metal adsorption

The results of the study showed that the highest adsorption percentage occurred at an epichlorohydrin concentration of 10%, with an adsorption rate of 82.98%. At this concentration, epichlorohydrin had reached an optimal amount to form effective crosslinking between chitosan and SBE. This resulted in a structure that provided numerous active sites capable of interacting with Fe(II) ions. At this stage, the porosity and availability of active surface areas in the composite were at their peak, allowing Fe(II) ions to be more easily trapped and adsorbed onto the adsorbent surface.

When the concentration of epichlorohydrin was further increased to 12.5%, saturation of the crosslinking process might have occurred. Fe(II) is a heavy metal that interacts with the $–NH_2$ groups of chitosan through coordination covalent bonding. The adsorbent's adsorption capacity decreases as the analyte concentration increases due to the system reaching a saturation point. At this stage, the adsorbent surface becomes fully occupied by analyte molecules, thus unable to adsorb additional analytes. The higher the concentration of epichlorohydrin used, the greater the chance of excessive interaction with chitosan, reducing the number of –OH groups available for adsorption, and thereby decreasing the adsorption percentage [39]. Conversely, when lower epichlorohydrin concentrations are used, there is less interaction with chitosan, leaving more –OH groups available for adsorption, which leads to an increase in adsorption percentage.

Determination of optimum pH for Fe(II) adsorption on SBE–chitosan crosslinked epichlorohydrin composites

The adsorption of metal ions is strongly influenced by the pH condition of the solution. In this study, the effect of pH on the adsorption of Fe(II) metal ions was tested at a concentration of 46.31 ppm with pH variations of 1, 3, 5, 7, and 9, and a contact time optimum for chitosan composites crosslinked with epichlorohydrin of 70 minutes [38]. The adsorption percentage results for each pH variation are shown in Figure 6.

The results of the study showed that the highest adsorption percentage occurred at pH 5, with

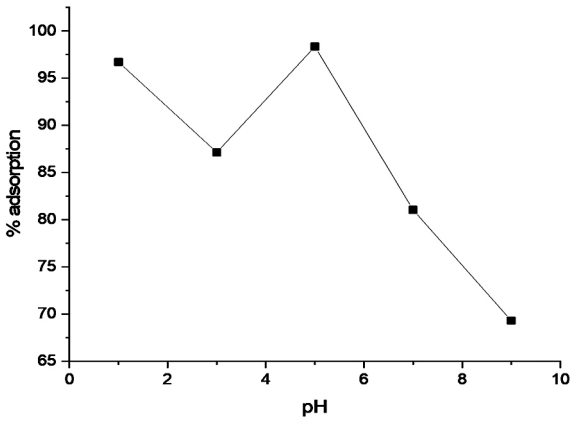

Figure 6. Graph of the effect of pH on Fe(II) metal adsorption on SBE-chitosan epichlorohydrin-crosslinked composite

an adsorption rate of 98.35%. Meanwhile, the lowest adsorption percentage was observed at pH 9, at only 69.29%. Based on Figure 6, the adsorption of Fe(II) metal ions in Fe(II) solution decreased from pH 1 to 3, and then increased from pH 3 to 5. This is due to the decreasing number of H^+ protons in the solution, allowing more Fe(II) ions to bind to the epichlorohydrin-crosslinked SBE-chitosan composite. The highest adsorption capacity was observed when the solution was at pH 5. This research is in line with adsorption of Cu(II), Cd(II) and Pb(II) the optimum pH values for the chitosan crosslinked with epichlorohydrin-triphosphate as the adsorbent were 6.0, 7.0 and 5.0 [16]. Adsorption of methylene blue and reactive red 120 dyes composite chitosan-epichlorohydrin/zeolite at pH 9 optimum for methylene blue and pH 6 for reactive red 120 [25].

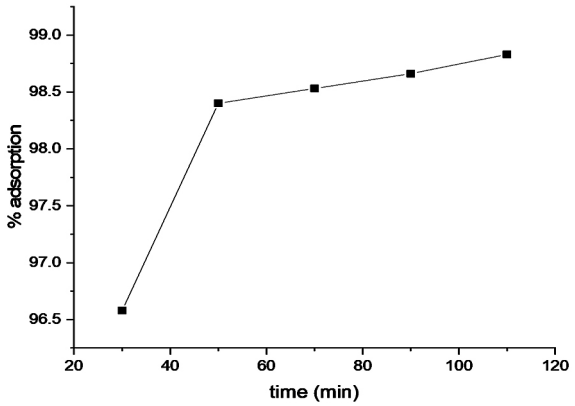

Figure 7. Effect of contact time on Fe(II) metal adsorption on epichlorohydrin crosslinked SBE-chitosan composite

In acidic conditions, there are a large number of H^+ protons that can bind to active groups ($–NH_2$) of chitosan and hydroxyl active groups, leading to competition between Fe(II) metal ions and hydrogen ions for access to the amine and hydroxyl active sites. H^+ protons, being harder Lewis acids than Fe(II), reduce the likelihood of Fe(II) binding to the adsorbent, thus decreasing the efficiency of Fe(II) ion removal. On the other hand, at pH > 8.5, Fe(II) precipitates completely As pH increases, the concentration of $OH^–$ ions also increases, strengthening the interaction between Fe(II) ions and $OH^–$ [40]. At pH values below 5, the high concentration of H^+ ions leads to protonation of the active groups in the epichlorohydrin-crosslinked SBE–chitosan adsorbent, particularly the protonation of $–NH_2$ (amine) to $–NH_3^+$ [41]. The higher the H^+ concentration, the greater the tendency for active group protonation, reducing Fe(II) adsorption due to the lack of free electron pairs available for bonding. At pH 5, Fe(II) is believed to have higher affinity for binding with the adsorbent's active groups, leading to increased ion adsorption. This result is consistent with finding [42]. Subsequently, the amount of Fe(II) adsorbed decreases as the solution pH continues to rise. This is due to the reduced solubility of the metal in solution, as Fe(II) remains in the form of $Fe(OH)_2$ [43]. As a result, the lone electron pairs on the active groups such as silanol, siloxane, amine, and hydroxyl groups on silica and chitosan are less effective in binding Fe(II).

Determination of the effect of contact time on Fe(II) adsorption on epichlorohydrin-crosslinked spent bleaching earth SBE-chitosan composite

Fe(II) metal adsorption on epichlorohydrin-crosslinked SBE–chitosan was conducted to determine the equilibrium contact time for adsorption at 30, 50, 70, 90, and 110 minutes. The variation in contact time is shown in Figure 7.

The results of the study show that optimal adsorption was already achieved at a contact time of 30 minutes, with no significant increase thereafter. The peak adsorption was reached at 110 minutes, with a value of 98.83%. Between 50 and 110 minutes, the adsorption level gradually increased. When adsorbate molecules come into contact with the surface of the adsorbent, some molecules bind to the surface, while others are repelled. At

the beginning of the contact time, the interaction is quite strong due to the abundance of available active sites on the adsorbent surface, resulting in a rapid increase in the adsorption rate. However, as contact time continues, the process approaches equilibrium and eventually stabilizes. Adsorption of humic acid from aqueous solutions on cross-linked chitosan–epichlorohydrin beads, after 50 min, it can be observed that the adsorption capacity remained constant and this implies that adsorption has reached the equilibrium state [27], removal of copper(II) ions from aqueous solution on chitosan and cross-linked chitosan beads [21], adsorption behaviour of Fe(II) and Fe(III) ions in aqueous solution on chitosan and cross-linked chitosan beads [38].

Determination of Fe(II) adsorption capacity on epichlorohydrin-crosslinked spent bleaching earth SBE-chitosan composite

The adsorption capacity of the epichlorohydrin-crosslinked SBE–chitosan composite for Fe(II) metal was determined at pH 5 and a contact time of 50 minutes. The equations used to describe the liquid adsorption process on solid surfaces are the Langmuir and Freundlich isotherms The use of adsorption isotherms aims to illustrate the interaction between the adsorbent

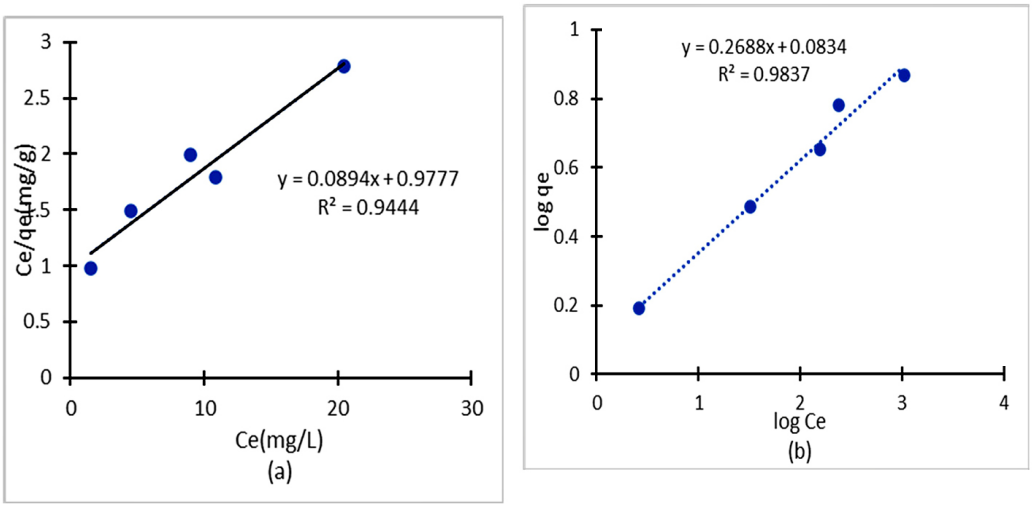

Figure 8. Results of the isotherm plots (a) Langmuir and (b) Freundlich for Fe(II) adsorption on spent bleaching earth SBE-chitosan crosslinked epichlorohydrin composite

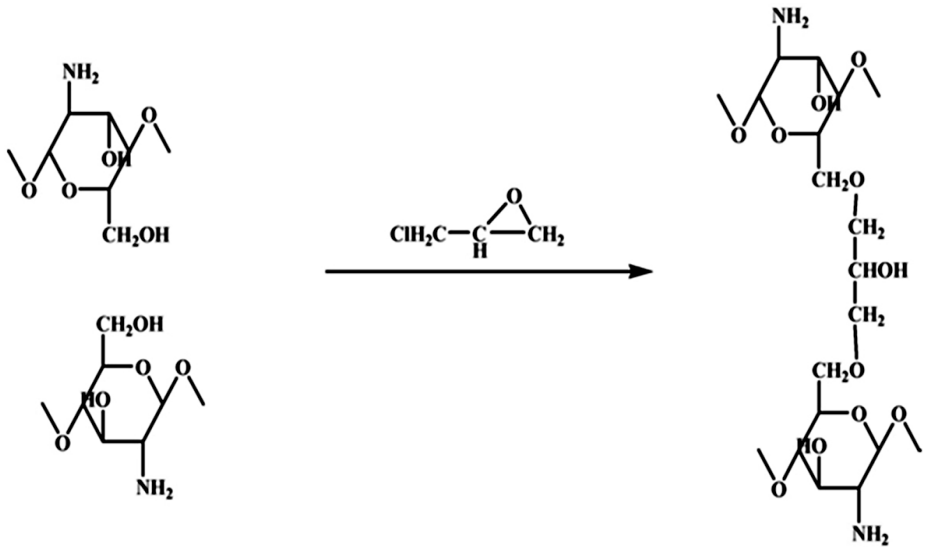

Figure 9. Reaction of chitosan and epichlorohydrin [49]

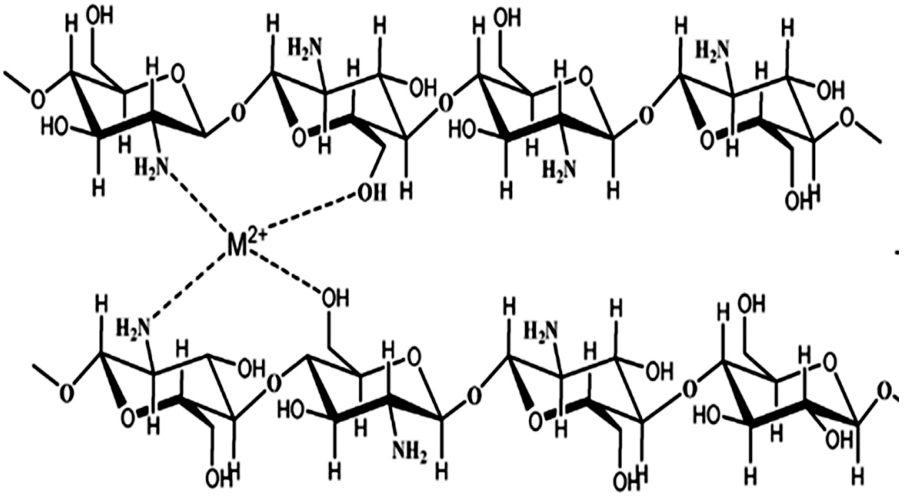

Figure 10. Interaction between metal and chitosan

and the adsorbate [27]. To observe the adsorption isotem that occurs in the adsorption process of the SBE chitosan ECH composite, it is calculated using equations 1 and 2. The adsorption isotherm plots of the Langmuir and Freundlich models for Fe(II) on spent bleaching earth (SBE)-chitosan crosslinked with epichlorohydrin composite can be seen in Figure 8.

Figure 8 shows that the adsorption follows the Langmuir and Freundlich isotherm, the maximum adsorption capacity determined from Langmuir model was 11.23 mgg^{-1}. This research is similar to the research on composites of activated carbon (AC) and AC/TiO_2) [44] and adsorption of yellow dye with a composite of natural clay and activated carbon [45], and adsorption of humic acid on crosslinked chitosan–epichlorohydrin(chitosan–ECH) beads [45]. The adsorption capacity value of the SBE-chitosan composite crosslinked with epichlorohydrin for Fe(II) is 11.23 mgg^{-1}. This adsorption capacity is smaller when compared to the adsorption capacity of chitosan crosslinked with epichlorohydrin for Fe(II) and Fe(III), where the obtained adsorption capacity was 57.47 mgg^{-1} [38]. Adsorption study conducted using low and high range concentration of methylene blue produced a maximum adsorption capacity 40.485 mgg^{-1} [26].

The high silica content in SBE makes it less effective in adsorbing metal ions such as Fe(II) [47]. In addition to these factors. the SBE-chitosan-epichlorohydrin composite that acts as a metal binder is the amine group of chitosan. Chitosan cross-linked with epicorohydrin as seen in Figure 9. causes the amine group of chitosan to decrease. so that its adsorption Fe capacity becomes low [27] and interaction between metal and chitosan can be seen in Figure 10 [48].

CONCLUSIONS

FTIR analysis results indicate that the soxhlet extraction and activation of SBE were effective in removing unsaturated vegetable oils and organic contaminants. In addition. FTIR also shows the successful formation of interactions between SBE-chitosan and epichlorohydrin during the preparation of the crosslinked composite. The successful adsorption of Fe(II) by this composite is characterized by the shift in wave numbers at specific functional groups. indicating interactions between Fe(II) and the composite. Based on the research conducted. it was found that the adsorption of Fe(II) on the SBE-chitosan composite crosslinked with epichlorohydrin showed optimal performance at pH 5. with equilibrium time achieved in 110 minutes. The adsorption follows the Langmuir and Freundlich isotherm, the maximum adsorption capacity determined from Langmuir model was 11.23 mgg^{-1}.

Acknowledgements

This research was financially supported by Lambung Mangkurat University Research Grant year 2023 with grant number 133/UN8.2/PG/2023.

REFFERENCES

1. González-Muñoz, M. J., Rodríguez, M. A., Luque, S., Álvarez, J. R. (2006). Recovery of heavy metals from metal industry waste waters by chemical precipitation and nanofiltration. *Desalination 200*, 742–744.
2. Wang, L., Tao, Y., Su, B., Wang, L., Liu, P. Contamination of Groundwater in the Sunan Coal Mine, China. (2022). *Toxics 10*(7), 390.
3. Wu, R. *et al.* (2022). Manganese pollution and its remediation: A review of biological removal and promising combination strategies. *Microorganisms 10*(12), 2411
4. Sebogodi, K. R., Johakimu, J. K., Sithole, B. B. (2020). Beneficiation of pulp mill waste green liquor dregs: Applications in treatment of acid mine drainage as new disposal solution in South Africa. *J. Clean. Prod. 246*, 118979.
5. Coil, D., Mckittrick, E., Mattox, A., Hoagland, N., Higman, B. H. (2014). Acid mine drainage. *Creat. Commons Attrib. Non- Commer.* 2–5
6. Utami, U. B. L., Susanto, H., Cahyono, B. (2020). Neutralization acid mine drainage (AMD) using NaOH at PT. Jorong Barutama Grestone, Tanah Laut, South Borneo. *IJCA (Indonesian J. Chem. Anal. 3*, 17–21.
7. *South Kalimantan Governor Regulation Number 36 Concerning Liquid Waste Quality Standards*. (2008).
8. Eko Saputro, K. *et al.* (2020). Reactivating adsorption capacities of spent bleaching earth for using in crude palm oil industry. *IOP Conf. Ser. Mater. Sci. Eng. 924*.
9. Pranowo, D., Dewanti, B. S. D., Fatimah, H., Setyawan, H. Y. (2020). Optimization of regeneration process of spent bleaching earth. *IOP Conf. Ser. Earth Environ. Sci. 524*.
10. Eko Saputro, K. *et al.* (2020). Reactivating adsorption capacities of spent bleaching earth for using in crude palm oil industry. *IOP Conf. Ser. Mater. Sci. Eng. 924*, 1–9.
11. Mu, B., Wang, A. (2018). Regeneration and recycling of spent bleaching earth. *Handb. Ecomater.* 1–21 doi:10.1007/978-3-319-48281-1_121-1.
12. Ali, M., Soud, S., Hameed, A. (2021). Chitosan hydrogel for removing of heavy metal ions from water: A review. *Eng. Technol. J. 39*, 1195–1205.
13. Zia, Q., Tabassum, M., Gong, H., Li, J. (2019). A review on chitosan for the removal of heavy metals ions. *J. Fiber Bioeng. Informatics 12*, 103–128.
14. Kayan, G. Ö., Kayan, A. (2021). Composite of natural polymers and their adsorbent properties on the dyes and heavy metal ions. *J. Polym. Environ. 29*, 3477–3496.
15. Akinyeye, J. O. (2016). Effect of chitosan powder prepared from snail shells to remove lead (II) ion and nickel (II) ion from aqueous solution and its adsorption isotherm model. *Am. J. Appl. Chem. 4*, 146.
16. Laus, R., Costa, T. G., Szpoganicz, B., Fávere, V. T. (2010). Adsorption and desorption of Cu(II), Cd(II) and Pb(II) ions using chitosan crosslinked with epichlorohydrin-triphosphate as the adsorbent. *J. Hazard. Mater. 183,* 233–241.
17. Gunawan, R., Shofiyani, A., Zaharah, T. A. T. (2017). He effect of activated carbon addition on the permeability properties of epichlorohydrin crosslinked chitosan composite membranes. *Jkk 7*, 1–9
18. Mathur, N. K., Narang, C. K. (1990). Chitin and chitosan, versatile polysaccharides from marine animals. *J. Chem. Educ. 67*, 938–942.
19. Wan Ngah, W. S., Kamari, A., Koay, Y. J. (2004). Equilibrium and kinetics studies of adsorption of copper (II) on chitosan and chitosan/PVA beads. *Int. J. Biol. Macromol. 34*, 155–161.
20. Ngah, W. S. W., Fatinathan, S. (2006). Chitosan flakes and chitosan-GLA beads for adsorption of p-nitrophenol in aqueous solution. *Colloids Surfaces A Physicochem. Eng. Asp. 277*, 214–222.
21. Patrulea, V. *et al.* (2013). Optimization of the Removal of Copper(II) Ions from Aqueous Solution on Chitosan and Cross-Linked Chitosan Beads. *BioResources 8*, 1147–1165.
22. Madjid, A. D. R., Nitsae, M., Sabarudin, A. (2018). Perbandingan butiran kitosan dengan pengikat silang epiklorohidrin (ECH) dan glutaraldehid (GLA): Karakterisasi dan kemampuan adsorpsi timbal (Pb). *Alchemy 6*, 29.
23. Ariyani, D., Cahaya, N., Mujiyanti, D. R. (2018). Pengaruh pH dan waktu kontak terhadap adsorpsi logam Zn(II) pada komposit arang eceng gondok termodifikasi kitosan-epiklorohidrin. *J. Kim. Val. 4*, 85–92.
24. Ariyani, D., Hilma, N.K., Utami, U.B.L.U., Trisno Santoso, D. R. M. (2023). Study effect of chitosan-epichlorohydrin macropore beads on decreasing the value of total dissolved solid (TDS) and dyes in sasirangan liquid waste treatment. *Indones. J. Chem. Res. 9*, 129–136.
25. Jawad, A. H., Abdulhameed, A. S., Reghioua, A., Yaseen, Z. M. (2020). Zwitterion composite chitosan-epichlorohydrin/zeolite for adsorption of methylene blue and reactive red 120 dyes. *Int. J. Biol. Macromol. 163,* 756–765.
26. Yulikasari, A., Nurhayati, E., Utama, W., Warmadewanthi, I. (2022). Characterization of spent bleaching earth as an adsorbent material for dye removal. *J. Ecol. Eng. 23*, 96–104.
27. Wan Ngah, W. S., Hanafiah, M. A. K. M., Yong, S. S. (2008). Adsorption of humic acid from aqueous solutions on crosslinked chitosan-epichlorohydrin beads: Kinetics and isotherm studies. *Colloids Surfaces B Biointerfaces 65*, 18–24.
28. Fajrudin, A., Supartono, Sumarni, W. (2016). The effect of nitric acid addition and calcination temperature on the reactivation of spent bleaching earth.

Indones. J. Chem. Sci. 5, 5–8.

29. Marrakchi, F., Hameed, B. H., Hummadi, E. H. (2020). Mesoporous biohybrid epichlorohydrin crosslinked chitosan/carbon–clay adsorbent for effective cationic and anionic dyes adsorption. *Int. J. Biol. Macromol. 163*, 1079–1086.
30. Naser, J., Avbenake, O. P., Dabai, F. N., Jibril, B. Y. (2021). Regeneration of spent bleaching earth and conversion of recovered oil to biodiesel. *Waste Manag. 126*, 258–265.
31. Dambuza, A., Mokolokolo, P. P., Makhatha, M. E., Sibeko, M. A. (2025). Chitosan-based materials as effective materials to remove pollutants. *Polymers 17*(18), 2447, 1–23.
32. Hu, S. zhong, Huang, T., Zhang, N., Lei, Zhou, Y., Wang, Y. (2022). Chitosan-assisted MOFs dispersion via covalent bonding interaction toward highly efficient removal of heavy metal ions from wastewater. *Carbohydr. Polym. 277,* 118809.
33. Firnanelty, Chadijah, S., Ratna, Nurhuda, S., Sittiama. (2021). Synthesis of chitosan-CuO composite and it's application as heavy metal adsorbent. *J. Phys. Conf. Ser. 1899.*
34. Merikhy, A., Heydari, A., Eskandari, H., Nematollahzadeh, A. (2019). Revalorization of spent bleaching earth a waste from vegetable oil refinery plant by an efficient solvent extraction system. *Waste and Biomass Valorization 10,* 3045–3055.
35. Silva, G. S., Oliveira, P. C., Giordani, D. S., De Castro, H. F. (2011). Chitosan/siloxane hybrid polymer: Synthesis, characterization and performance as a support for immobilizing enzyme. *J. Braz. Chem. Soc. 22*, 1407–1417.
36. Zamrodah, Y. (2016). The use of epichlorohydrin in improving the stability of cross-linked chitosan adsorbents and cobalt-ionic printed chitosan. *Al-Kimia 15*, 1–23.
37. Suhartini, M. (2013). Modification of banana peel waste for adsorbent of Mn(II) and Cr(VI) metal ions. *Indones. J. Mater. Sci. 14,* 229–234.
38. Ngah, W. S. W., Ab Ghani, S., Kamari, A. (2005). Adsorption behaviour of Fe(II) and Fe(III) ions in aqueous solution on chitosan and cross-linked chitosan beads. *Bioresour. Technol. 96*, 443–450.
39. Wijayanti, I. L. D., Mahatmanti, F. W. (2022). Synthesis of chitosan/activated carbon composite beads as an adsorbent of Pb(II) and Cu(II) ions in aqueous solution: A review. *Indones. J. Chem. Sci. 11*, 190–197.
40. Rahayu, P., Khabibi, K. (2016). Adsorption of nickel(II) metal ions by tripolyphosphate-modified chitosan. *J. Kim. Sains dan Apl. 19*, 21.
41. Fajarwati, F. I., Kurniawan, M. A., Fatima, M. N. & Fikrina, R. Removal of Dyes Using Chitosan-Alginate Polyelectrolyte Complex. *JPSCR J. Pharm. Sci. Clin. Res. 3*, 36 (2018).
42. Budnyak, T., Tertykh, V., Yanovska, E. (2014). Ant silicio oksido paviršiaus imobilizuotas chitozanas nuotekoms valyti. *Medziagotyra 20*, 177–182.
43. Amelia, H., Fitria, R., Sunardi, S. (2023). Isothermal study of methylene blue adsorption on sago peel (metroxylon sagu) biochar. *Justek J. Sains dan Teknol. 6*, 135.
44. Mohamad Zain, N. *et al.* (2021). Synergistic effect of TiO_2 size on activated carbon composites for ruthenium n-3 dye adsorption and photocatalytic degradation in wastewater treatment. *Environ. Nanotechnology, Monit. Manag*. *16*, 100567.
45. Ayisha Sidiqua, M., Priya, V. S. (2021). Removal of yellow dye using composite binded adsorbent developed using natural clay and activated carbon from sapindus seed. *Biocatal. Agric. Biotechnol. 33*,
46. Govindan, S., Nivethaa, E. A. K., Saravanan, R., Narayanan, V., Stephen, A. (2012). Synthesis and characterization of Chitosan–Silver nanocomposite. *Appl. Nanosci. 2*, 299–303.
47. Buhani, B., Narsito, N., Nuryono, N., Kunarti, E. S. (2010). Amino and mercapto-silica hybrid for Cd(II) adsorption in aqueous solution. *Indones. J. Chem. 9*, 170–176.
48. Chen, A. H., Yang, C. Y., Chen, C. Y., Chen, C. Y., Chen, C. W. (2009). The chemically crosslinked metal-complexed chitosans for comparative adsorptions of Cu(II), Zn(II), Ni(II) and Pb(II) ions in aqueous medium. *J. Hazard. Mater. 163*, 1068–1075.
49. Chen, A. H., Liu, S. C., Chen, C. Y., Chen, C. Y. (2008). Comparative adsorption of Cu(II), Zn(II), and Pb(II) ions in aqueous solution on the crosslinked chitosan with epichlorohydrin. *J. Hazard. Mater. 154*, 184–191.